

Tensor effects on the proton sd states in neutron-rich Ca isotopes and bubble structure of exotic nuclei

Y. Z. Wang (王艳召),^{1,*} J. Z. Gu (顾建中),^{1,2,†} X. Z. Zhang (张锡珍),¹ and J. M. Dong (董建敏)^{1,3}

¹China Institute of Atomic Energy, P. O. Box 275 (10), Beijing 102413, China

²Center of Theoretical Nuclear Physics, National Laboratory of Heavy Ion Accelerator of Lanzhou, Lanzhou 730000, China

³School of Nuclear Science and Technology, Lanzhou University, Lanzhou 730000, China

(Received 20 July 2011; revised manuscript received 17 October 2011; published 31 October 2011)

In the framework of the Hartree-Fock-Bogoliubov (HFB) approach with Skyrme interactions SLy5+T, SLy5+T_w and several sets of the *TIJ* parametrizations, the evolution of the proton single-particle energy difference between the $2s_{1/2}$ and $1d_{3/2}$ orbits in Ca isotopes is investigated for the cases with and without the tensor force. It is shown that the energy difference evolution trends by using different Skyrme interactions without the tensor force are similar to each other. However, the energy differences are obviously influenced by the tensor force. Meanwhile, it is found that the inversion between the two orbits ($2s_{1/2}$ - $1d_{3/2}$ inversion) induced by the tensor force occurs around ⁴⁸Ca (by SLy5+T_w) as well as in the nuclei very far from the stability. We understand the inversion phenomenon by analyzing the tensor contributions to the spin-orbit potentials and the radial wave functions of the two orbits. Finally, the proton density distributions of ⁴⁶Ar and ²⁰⁶Hg are calculated by using several sets of Skyrme interactions with and without the tensor component. It is found that the parametrization SLy5+T_w favors the bubble structure of ⁴⁶Ar resulting from the $2s_{1/2}$ - $1d_{3/2}$ inversion. However, for ²⁰⁶Hg any tensor parametrizations do not favor its bubble structure.

DOI: [10.1103/PhysRevC.84.044333](https://doi.org/10.1103/PhysRevC.84.044333)

PACS number(s): 21.10.Pc, 21.30.Fe, 21.60.Jz

I. INTRODUCTION

In nucleon-nucleon (*NN*) interaction the tensor force is an important ingredient [1,2], which has a crucial influence on the nuclear structure, such as the single-particle spectrum [3], nuclear matter with realistic potentials [4], nuclear deformation [5], and nuclear multipole giant resonances [6,7]. In the 1970s, some nuclear physicists pointed out that the tensor part of the nucleon-nucleon effective interaction has an important role in the spin-orbit splitting of the Hartree-Fock (HF) single-particle spectrum [8–12]. In fact, in the self-consistent mean-field theory, the effective zero-range nonlocal interaction proposed by Skyrme contains a zero-range tensor force [13,14]. However, the tensor force of the Skyrme interaction was neglected in the later calculations of self-consistent mean-field models. In the early work of Stancu *et al.* [3], they studied the tensor effects on the spin-orbit splitting by adding the tensor force in a perturbative way in the 1970s. After that most of the Skyrme forces were fitted without considering the tensor contribution except for the work done by Tondeur, and Liu *et al.* [15,16]. Until recent years, there was only very little development of the tensor force. People recently studied the shell structure of exotic nuclei based on the shell model by taking into account the tensor force, showing that the tensor force plays a crucial role in the evolution of shell structure [17–20]. Then, for the nuclei far from the stability, the study of the shell evolution and modification of some magic numbers induced by the tensor effects within various self-consistent mean-field approaches becomes an interesting subject in nuclear structure study [21–28]. For example, in the Skyrme-HF theory, the

tensor force was usually added perturbatively into the existing standard parametrization SLy5. The calculations showed that some features on the evolution of the single-particle states are described successfully by taking into account the tensor force [22–25,28].

It is well known that the single-particle states of exotic nuclei are quite different from those of stable nuclei. For instance, studies indicated that the inversion phenomenon of *s* and *d* states may occur in some neutron-rich nuclei [29–31]. So to speak, the $2s_{1/2}$ - $1d_{3/2}$ inversion phenomenon was predicted in ⁴⁸Ca within the relativistic mean-field (RMF) approach [32]. The experimental signals for the inversion phenomenon was found by measuring the proton single-particle spectrum of ⁴⁸Ca [33]. The fact that the ground state of ⁴⁷K is $1/2^+$ with a large spectroscopic factor [34] also indicates that there is $2s_{1/2}$ - $1d_{3/2}$ inversion in the proton single-particle spectrum of ⁴⁸Ca. Thus the study of the inversion phenomenon for the single-particle states of exotic nuclei becomes an attractive topic. In the 1970s, people analyzed the problem of $2s_{1/2}$ - $1d_{3/2}$ inversion of the proton states obtained by the HF+BCS [35] approach with an interaction derived from a *G* matrix [36]. It was shown that ³⁶Ar was a candidate for this inversion. But the Skyrme interactions could not lead to any inversion in this nucleus. Recently, Grasso *et al.* analyzed the evolution of the *s*-*d* proton single-particle states in Ca isotopes and a possible $2s_{1/2}$ - $1d_{3/2}$ inversion within the Skyrme-HF method [37]. In their analysis, all factors including the kinetic, central, spin-orbit, and tensor terms, which may modify the single-particle energies were discussed. It was shown that the tensor effect considerably favors the inversion of the two proton states in ⁴⁸Ca. Nevertheless, the pairing correlation was neglected in their work so that the proton single-particle states of some open-shell nuclei could not be described properly. In addition, in the studies of the tensor effect, they just used one set of

* yanzhaowang09@126.com

† gujianzhong2000@yahoo.com.cn

Skyrme interaction SLy5+T. So far, people have developed many sets of Skyrme effective interactions including the tensor terms in addition to SLy5+T, such as SLy5+T_w [3,6], the *TIJ* parametrizations [38,39]. Thus it is worth revisiting the problem to explore the evolution of the *sd* states and the inversion phenomena of the open-shell nuclei by using more Skyrme interactions with the tensor force. This is the first motivation of this article. Meanwhile, the bubble effects of exotic nuclei has attracted much attention [40–42]. The bubble nuclei are characterized by a depleted central density. This effect originates from a very low occupation probability of the *s*_{1/2} state: The absence of the *l*=0 contribution leads to a strong drop of the density in the center of the nuclei. Corresponding studies indicate that the bubble effects require some conditions, such as weak or low pairing and deformation effects [43], to ensure a low occupation probability of the *s* state. Bubble nuclei were predicted in various mass regions [32,40–43]. For ⁴⁶Ar the *s*_{1/2} proton orbit is predicted to move significantly above the *d*_{3/2} state [32], that is, the inversion of *s* and *d* states, which is the key factor for the bubble formation. For heavy nucleus ²⁰⁶Hg its bubble structure is attributed to the inversion between *s* and *h* states [32]. Therefore, it is interesting to study the tensor effects on the bubble structure. This is the second motivation of this article. It is well known that the Skyrme parametrizations are suitable for investigating bulk properties of nuclei in the framework of the HFB theory [44–47], and with the pairing correlation taken into account by the Bogoliubov transformation, the nuclear properties near drip lines can be better described than those with the BCS approximation. Driven by the two motivations mentioned above, we investigate the tensor effects on the evolution of the proton single-particle states 2*s*_{1/2} and 1*d*_{3/2}, the inversion phenomenon of the two states in Ca isotopes, and the bubble structure of ⁴⁶Ar and ²⁰⁶Hg by using the HFB theory with Skyrme interactions SLy+T, SLy5+T_w, and several sets of the *TIJ* parametrizations. This article is organized as follows. In Sec. II a theoretical framework is introduced. The numerical results and corresponding discussions are given in Sec. III. The conclusions are drawn in Sec. IV.

II. THEORETICAL FRAMEWORK

The triplet-even and triple-odd zero-range tensor terms of Skyrme force are expressed as

$$\begin{aligned}
 v_T = & \frac{T}{2} \left[(\sigma_1 \cdot \mathbf{k}')(\sigma_2 \cdot \mathbf{k}') - \frac{1}{3}(\sigma_1 \cdot \sigma_2)\mathbf{k}^2 \right] \delta(\mathbf{r}_1 - \mathbf{r}_2) \\
 & + \frac{T}{2} \delta(\mathbf{r}_1 - \mathbf{r}_2) \left[(\sigma_1 \cdot \mathbf{k})(\sigma_2 \cdot \mathbf{k}) - \frac{1}{3}(\sigma_1 \cdot \sigma_2)\mathbf{k}^2 \right] \\
 & + U[(\sigma_1 \cdot \mathbf{k}')\delta(\mathbf{r}_1 - \mathbf{r}_2)(\sigma_2 \cdot \mathbf{k}) \\
 & - \frac{1}{3}U(\sigma_1 \cdot \sigma_2) \times [\mathbf{k}' \cdot \delta(\mathbf{r}_1 - \mathbf{r}_2)\mathbf{k}], \quad (\text{II.1})
 \end{aligned}$$

where the operator $\mathbf{k} = (\nabla_1 - \nabla_2)/2i$ acts on the right and $\mathbf{k}' = -(\nabla_1 - \nabla_2)/2i$ acts on the left. The coupling constants *T* and *U* are the strengths of the triplet-even and triple-odd tensor interactions, respectively. The tensor force and central

exchange term lead to a contribution to the energy density,

$$\Delta H(\mathbf{r}) = \frac{1}{2}\alpha(J_n^2 + J_p^2) + \beta J_n J_p. \quad (\text{II.2})$$

The spin-orbit potential with the central exchange and tensor term is given by

$$U_{\text{s.o.}}^q = \frac{W_0}{2r} \left(2 \frac{d\rho_q}{dr} + \frac{d\rho_{q'}}{dr} \right) + \left(\alpha \frac{J_q}{r} + \beta \frac{J_{q'}}{r} \right), \quad (\text{II.3})$$

where $J_{q(q')}(r)$ is the proton or neutron spin-orbit density defined as

$$\begin{aligned}
 J_{q(q')}(r) = & \frac{1}{4\pi r^3} \sum_i (2j_i + 1) \\
 & \times \left[j_i(j_i + 1) - l_i(l_i + 1) - \frac{3}{4} \right] R_i^2(r). \quad (\text{II.4})
 \end{aligned}$$

In this expression *q* stands for neutrons (protons) and *q'* for protons (neutrons), where *i* = *n*, *l*, *j* runs over all states having the given *q* (*q'*), and $R_i(r)$ is the radial part of the wave function.

The terms in the first bracket of Eq. (3) come from the Skyrme spin-orbit interaction, and the terms in the second bracket include both the central exchange and the tensor contributions. In Eqs. (2) and (3), $\alpha = \alpha_C + \alpha_T$ and $\beta = \beta_C + \beta_T$. The coupling constants can be determined as follows [10,13,14,47]:

$$\begin{aligned}
 \alpha_C = & \frac{1}{8}(t_1 - t_2) - \frac{1}{8}(t_1 x_1 + t_2 x_2), \\
 \beta_C = & -\frac{1}{8}(t_1 x_1 + t_2 x_2), \quad (\text{II.5})
 \end{aligned}$$

$$\begin{aligned}
 \alpha_T = & \frac{5}{12}U, \\
 \beta_T = & \frac{5}{24}(T + U). \quad (\text{II.6})
 \end{aligned}$$

For the convenience of the following discussion, we rewrite Eq. (3) in the following form:

$$\begin{aligned}
 U_{\text{s.o.}}^q = & U_\rho + U_C + U_T \\
 = & \frac{W_0}{2r} \left(2 \frac{d\rho_q}{dr} + \frac{d\rho_{q'}}{dr} \right) \\
 & + \left(\alpha_C \frac{J_q}{r} + \beta_C \frac{J_{q'}}{r} \right) + \left(\alpha_T \frac{J_q}{r} + \beta_T \frac{J_{q'}}{r} \right). \quad (\text{II.7})
 \end{aligned}$$

In this work, all calculations were performed using the HFBRAD code [44] with the Skyrme force in the particle-hole channel. In the pairing channel, we use the mixing pairing interaction, which is written as

$$V = \left(t'_0 + \frac{t'_3}{6} \rho^{\gamma'} \right) \delta, \quad (\text{II.8})$$

where $t'_3 = -18.75t'_0$, $\gamma' = 1$, and t'_0 is an adjusted parameter, which can be determined by the empirical pairing gaps. The box and mesh sizes are selected as 30 fm and 0.1 fm, respectively.

III. RESULTS AND DISCUSSIONS

We have performed systematic calculations for the proton single-particle energy difference between the 2*s*_{1/2} and 1*d*_{3/2} states in Ca isotopes by using the HFBRAD code with the

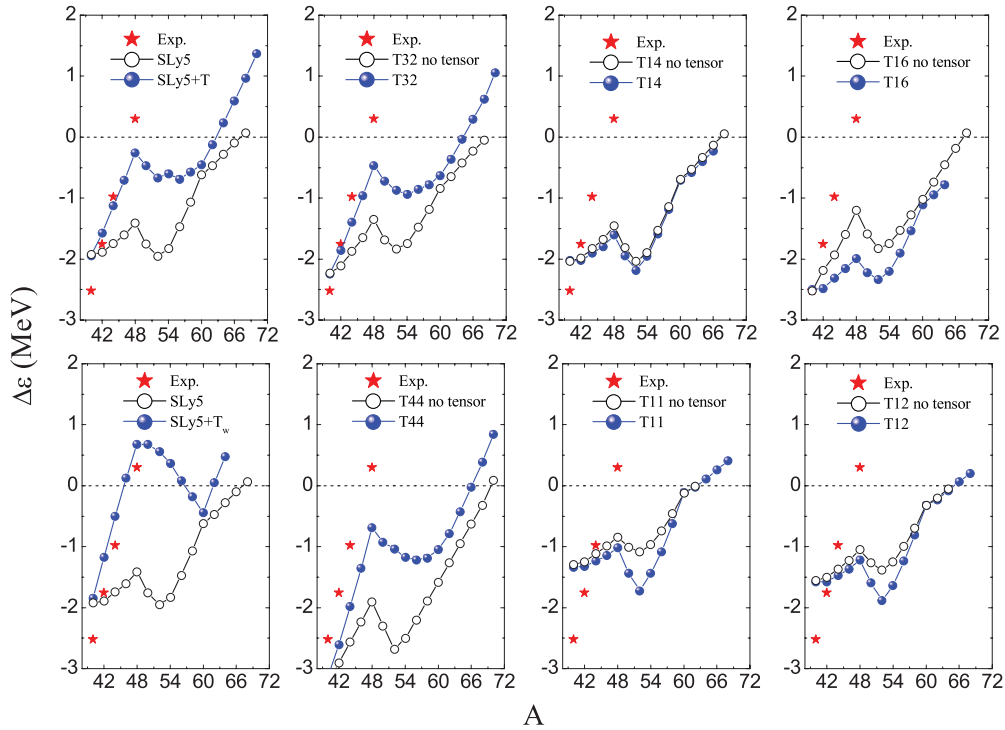


FIG. 1. (Color online) Comparison between the experimental data and the calculated energy differences of the proton single-particle states $2s_{1/2}$ and $1d_{3/2}$ in Ca isotopes in the cases with and without tensor force.

Skyrme interactions SLy5+T, SLy5+ T_w , and several sets of the T_{IJ} parametrizations. Note that the single-particle spectra are computed in the canonical basis. The calculated results with and without the tensor force and available experimental data as functions of the mass number A are plotted in Fig. 1. The experimental data is taken from Ref. [33,48]. From Fig. 1, we can see that all Skyrme interactions without the tensor force give similar evolution trends, which is consistent with those in Ref. [37]. This is because the fillings of neutron orbits are the same although the interactions are different from each other. As can be seen from Fig. 1, the single-particle energy differences of the s - d states for the nuclei $^{40,60}\text{Ca}$ are not influenced by the tensor force because they are the spin-saturated nuclei for both protons and neutrons. The tensor contributions to the energy differences almost vanish. But the small changes in the energy differences of the nucleus ^{60}Ca can be seen from the pairing interaction. For other isotopes, the energy differences are more or less influenced by the tensor force. According to the comparisons of the calculated results with different Skyrme interactions in Fig. 1, it is not difficult to find that there are the following interesting features:

(i) The energy difference evolution trends of the two states are similar to each other for SLy5+T, T32, and T44. The values of energy differences with the tensor force are larger than the ones without the tensor force for these interactions.

(ii) The evolution trends are similar to each other for the T1X (T11, T12, T14, T16) interactions. The energy difference values with the tensor force are smaller than those without the tensor effect.

(iii) The Skyrme interaction with the tensor force SLy5+ T_w leads to the $2s_{1/2}$ - $1d_{3/2}$ inversion near ^{48}Ca . For the very

neutron-rich nuclei, there are the inversion phenomena because of the tensor effect.

As to the evolution tendency varying with the mass number A induced by the tensor force for each interaction, it is well described by the monopole effect proposed by Otsuka *et al.* [17–19]. Here we will not redescribe the effect to explain the single-particle spectrum shifts. We now focus on discussing the features mentioned above by taking $^{48,64}\text{Ca}$ as an example using the spin-orbit potentials and the radial wave functions of $2s_{1/2}$ and $1d_{3/2}$ states. The proton spin-orbit potentials and the squared radial wave functions with the interactions SLy5+T, SLy5+ T_w , and T16 as functions of the radial distance r for $^{48,64}\text{Ca}$ are plotted in Fig. 2.

From Fig. 2, one can see that the tensor contribution to the spin-orbit potential U_T with SLy5+T of $^{48,64}\text{Ca}$ varies with r positively. This is because Ca isotopes except for $^{48,64}\text{Ca}$ are the spin-saturated nuclei for protons. Thus the tensor effects are practically attributable only to the fillings of neutron orbits so that one cannot obtain the contributions from the total proton spin current density J_p . In our calculations, the total neutron spin current density J_n is positive. Therefore, the tensor contribution to the spin-orbit potential is only relevant to the parameter β_T . The values of β_T for different versions of Skyrme forces are listed in Table I. From Table I, one can see that $\beta_T = 100.0 \text{ MeV fm}^5$ so that the tensor effect gives a positive contribution to U_T . For T32 and T44, the situations are similar to that with SLy5+T because the β_T values with T32 and T44 are 79.5 MeV fm^5 and 112.8 MeV fm^5 , respectively. Thus the first feature is explained by the positive U_T . For T16 parametrization the β_T value is -69.1 MeV fm^5 , which makes the U_T of $^{48,64}\text{Ca}$ negative. It can be seen from the

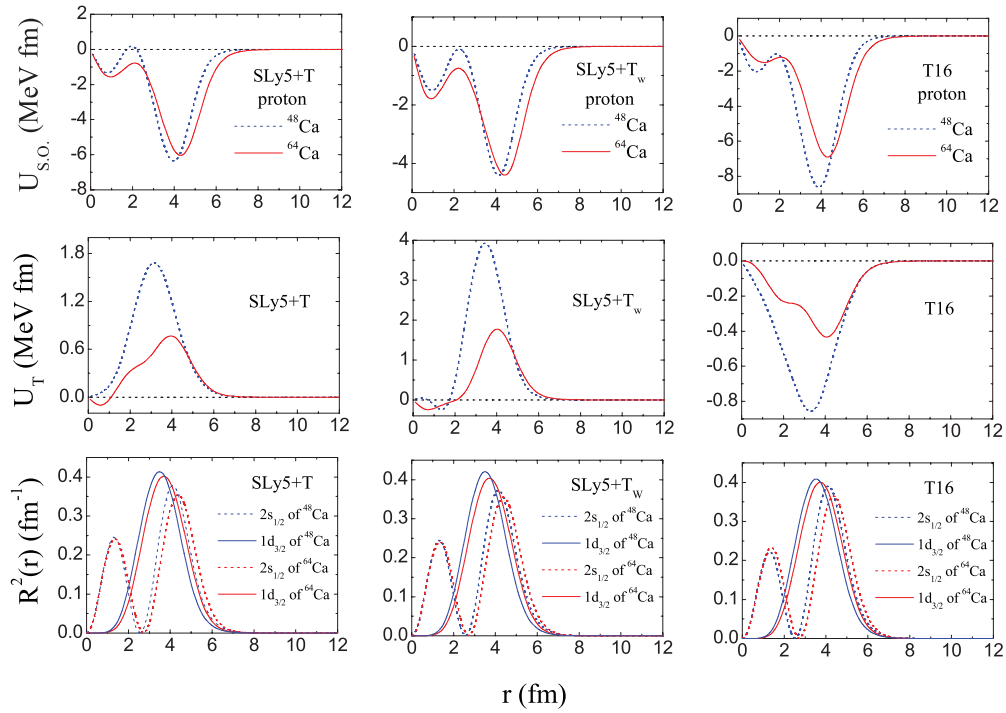


FIG. 2. (Color online) Proton spin-orbit potentials and the squared radial wave functions of the $2s_{1/2}$ and $1d_{3/2}$ orbits for $^{48,64}\text{Ca}$ with Skyrme interactions SLy5+T, SLy5+T_w, and T16.

third column in Fig. 2. For other T1X parametrizations the β_T values are all negative, which leads to the negative U_T . Thus the evolutions of s - d states with the tensor effects by using the T1X interactions are opposite to those of SLy5+T, T32, and T44. So the second feature is also interpreted well by the analysis mentioned above. The similar mechanism was already described in our previous work [28]. In addition, from Fig. 2 one can see that the wave functions of $1d_{3/2}$ orbit corresponding interactions SLy5+T, SLy5+T_w, and T16 and the total potential $U_{s.o.}$ are peaked almost at the same r . This indicates that the $1d_{3/2}$ orbit is strongly modified by the tensor contribution. However, because the wave functions of $2s_{1/2}$ have nodes in the region between 2.5 and 3.0 fm, this orbit is not sensitive to the tensor effect. To make the conclusion clearer, the proton single-particle spectra of $^{48,64}\text{Ca}$ with and without the tensor force are plotted in Fig. 3. As can be seen

from Fig. 3, the single-particle energies of the $1d_{3/2}$ orbits for $^{48,64}\text{Ca}$ are indeed changed evidently by the tensor force. However, there are almost no changes in the $2s_{1/2}$ energies with the tensor effect.

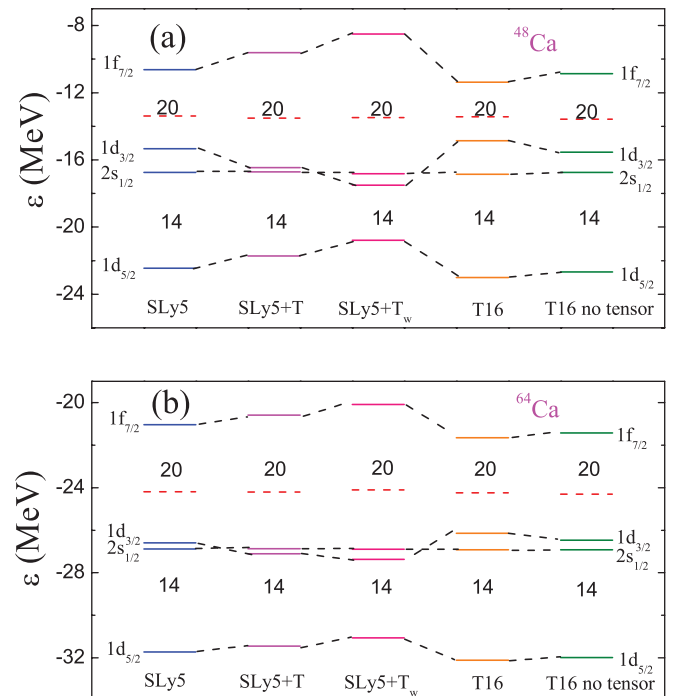


FIG. 3. (Color online) Proton single-particle energies of $^{48,64}\text{Ca}$ with Skyrme interactions SLy5, SLy5+T, SLy5+T_w, and T16.

TABLE I. The tensor parametrizations α_T and β_T corresponding different versions of Skyrme interactions. All values are in units of MeV fm⁵.

Forces	α_T	β_T
SLy5+T	-170.0	100.0
SLy5+T _w	134.76	238.2
T32	-96.5	79.5
T44	9.0	112.8
T11	-142.8	-17.5
T12	-82.6	-17.1
T14	38.5	-15.2
T16	131.2	-69.1

In this paragraph we will analyze the reason for the third feature induced by the tensor force. As the analysis mentioned above, we can get positive U_T with SLy5+T, T32, and T44. The single-particle energy of $1d_{3/2}$ orbit is lowered by the positive U_T . As a result, the two orbits stay very close, which can be seen clearly from Fig. 3(a) according to the comparison between the theoretical spectrum with SLy5 and that with SLy5+T. As to SLy5+ T_w , its β_T value is about twice as large as the one with SLy5+T so that one can obtain a larger U_T with SLy5+ T_w . The peak value of U_T with SLy5+ T_w for ^{48}Ca is roughly equivalent to the absolute value of the total spin-orbit potential $U_{s.o.}$. Hence, such a large U_T with SLy5+ T_w can make the single-particle energy of $1d_{3/2}$ orbit drop sharply so as to exceed the $2s_{1/2}$ orbit. As a result, the $2s_{1/2}$ - $1d_{3/2}$ inversion occurs. For the very neutron-rich nuclei, the tensor effect in SLy5+T, T32, and T44 interactions can be strong enough to drive the inversion. Thus the two-state inversion surely occurs within SLy5+ T_w , which can be seen clearly from Fig. 3(b). About the T1X forces, for example, the T16 interaction, the $1d_{3/2}$ orbit is pushed up by the tensor force, which can be seen from Fig. 3. The $2s_{1/2}$ - $1d_{3/2}$ energy difference with the T16 parametrization becomes smaller than that with this interaction not including the tensor force. Thus the T1X interactions do not favor the $2s_{1/2}$ - $1d_{3/2}$ inversion phenomenon near ^{48}Ca .

Some corresponding studies suggest that the $2s_{1/2}$ - $1d_{3/2}$ inversion phenomena exist in many neutron-rich isotopes [32,36,40,43,49]. For example, the proton $2s_{1/2}$ - $1d_{3/2}$ inversion in ^{46}Ar , which serves a key factor for the proton bubble formation [32,40,43]. The study of bubble nuclei is interesting because the future experimental data will be accessible with the help of the radioactive ion beams and the exotic nucleus experiments. Furthermore this is a big challenge and a severe test for theoretical studies. In Fig. 4, we show the proton density distributions of ^{46}Ar by using different versions of Skyrme interactions with and without the tensor force. From Fig. 4, one can see that the tensor force has almost no influence on the central values of the proton density except for the interaction SLy5+ T_w . The central density decreases obviously in terms of the interaction SLy5+ T_w . To explain the phenomenon more clearly, we show the proton single-particle energies of ^{46}Ar

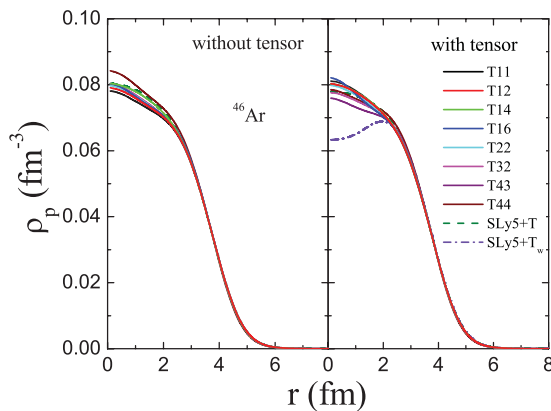


FIG. 4. (Color online) Proton density distributions of ^{46}Ar corresponding different Skyrme interactions with and without the tensor force.

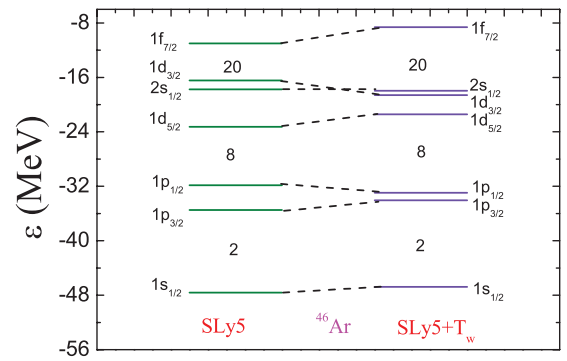


FIG. 5. (Color online) Proton single-particle spectrum of ^{46}Ar with SLy5 and SLy5+ T_w interactions.

with the parametrizations SLy5 and SLy5+ T_w in Fig. 5. As can be seen from Fig. 5, the $2s_{1/2}$ - $1d_{3/2}$ inversion phenomenon is found within the parametrization SLy5+ T_w . The inversion mechanism is similar to the situation of ^{48}Ca with SLy5+ T_w . Because ^{46}Ar is a spin-unsaturated nucleus for both proton and neutron, the parameters α_T , β_T and the spin current densities J_n , J_p have contributions to U_T . In our calculations, parameters α_T , β_T and the spin current densities J_n , J_p are all positive. Thus one can get the positive U_T , whose peak value is very large. The $1d_{3/2}$ orbit drops obviously being a big U_T , but the $2s_{1/2}$ orbit is almost unchanged. As a result, the $2s_{1/2}$ - $1d_{3/2}$ inversion occurs and the occupation probability of $2s_{1/2}$ orbit decreases. Therefore, the proton density profile presents a depletion in the interior of the nucleus. According to the analysis mentioned above, it is not difficult to conclude that the parametrization SLy5+ T_w favors the bubble effect of ^{46}Ar . Previous studies suggested that the pairing effect may hinder the bubble formation because scattered pairs could populate the $s_{1/2}$ state, decreasing the depletion in the center of the nucleus [40,42]. Thus the bubble formation of ^{46}Ar originates from the competition between the tensor and pairing effects. Our work also indicates that the role of the tensor effect from SLy5+ T_w plays more importantly than that of the pairing effect in the bubble formation of ^{46}Ar .

Recently, Gade *et al.* [49] discussed the importance of the tensor effects on the proton single-particle gap evolution of odd-mass K, Cl, and P isotopes for $N = 20$ –28 with the shell model. The $2s_{1/2}$ - $1d_{3/2}$ inversion was found in K and Cl isotopes for $N = 28$, which supports our calculated results with SLy5+ T_w . This indicates that the proton sd inversion exists widely in this mass region. In addition, a composite model based on the HF for central, G matrix for spin-orbit, and $\pi + \rho$ for tensor contributions was proposed for the evolution between the $s_{1/2}$ and $d_{3/2}$ states. The calculated results are in reasonable agreement with the experimental data. Just like their idea, the SLy5+ T_w interaction could be seen as a composite model because the tensor force in SLy5+ T_w is obtained by the low- q limit of the G -matrix calculations [3], which is added perturbatively to the existing force SLy5. Namely, the SLy5 interaction and the tensor component in SLy5+ T_w interaction have different sources. Each component in different NN interactions has its reasonableness and advantage. Combining the advantages of the components from

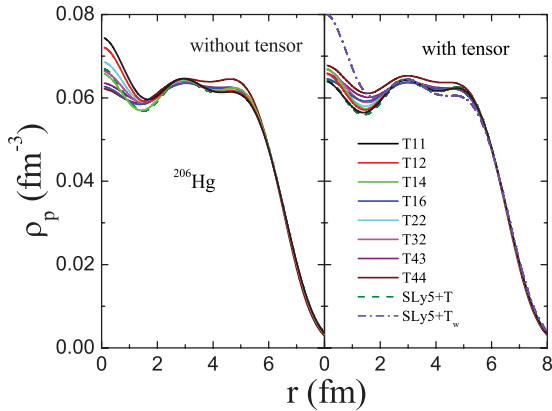


FIG. 6. (Color online) Proton density distributions of ^{206}Hg corresponding different Skyrme interactions with and without the tensor force.

different NN interactions we can understand the exotic nuclear structure deeply although the composite approach is not so self-consistent.

The bubble effects were predicted in some heavy nuclei [32,41], but their bubble formation mechanism is different from that of ^{46}Ar . For example, ^{206}Hg was a predicted proton bubble nucleus [32]. Its central proton density depends on the occupation probability of $3s_{1/2}$ orbit. According to our calculations, it is found that the $3s_{1/2}-1h_{11/2}$ inversion exists for all the Skyrme interactions except for $\text{SLy5}+T_w$. Nevertheless, there is high occupation probability in the $3s_{1/2}$ orbit because of the pairing effect. As a result, the bubble formation of ^{206}Hg is suppressed. The calculated proton density distributions of ^{206}Hg by using several sets of Skyrme interactions with and without the tensor force are plotted in Fig. 6. From Fig. 6, one can see that the bubble effects are not evident with and without the tensor force. In addition, one can see that the $\text{SLy5}+T_w$ parametrization enhances the central density. This is because the $\text{SLy5}+T_w$ parametrization prevents the $3s_{1/2}-1h_{11/2}$ inversion so that the protons are almost fully filled in the $3s_{1/2}$ orbit. According to the discussions mentioned above, it is not difficult to conclude that none of the tensor parametrizations favors the bubble structure of ^{206}Hg .

IV. CONCLUSIONS

In this paper the tensor effects on the evolution of the proton single-particle energy difference between the $2s_{1/2}$ and $1d_{3/2}$ states in Ca isotopes have been investigated with the Skyrme interactions $\text{SLy5}+T$, $\text{SLy5}+T_w$, and several sets of the T_{IJ} parametrizations in the framework of the HFB approach. It was shown that the evolution trends are similar to each other by using different Skyrme interactions without the tensor force. However, the energy differences between the two states are influenced by the tensor force: First, the evolution trends of the two states are similar to each other for $\text{SLy5}+T$, T32, and T44, and the values of energy differences with the tensor force are larger than the ones without the tensor force for these interactions; second, the evolution trends are similar to each other for the T_{IX} interactions. The energy difference values with the tensor force are smaller than those without the tensor force. Meanwhile, we found that the inversion phenomenon of the two states induced by the tensor force occurs around ^{48}Ca (by $\text{SLy5}+T_w$) as well as in the nuclei very far from the stability. For these features, we have analyzed the tensor contributions to the spin-orbit potentials and the radial wave functions of the two orbits. In addition, the tensor effects on the proton bubble structure of ^{46}Ar and ^{206}Hg were studied. It is found that the parametrization $\text{SLy5}+T_w$ favors the bubble effect of ^{46}Ar because of the $2s_{1/2}-1d_{3/2}$ inversion. For ^{206}Hg , any tensor parametrizations do not favor its bubble structure. Finally, we would point out that the giant resonance modes of the bubble nuclei could be different from those of normal nuclei because of their exotic nuclear structure. Thus, it is interesting to study the giant resonances of the bubble nuclei, which is a work in progress.

ACKNOWLEDGMENTS

Y.Z.W. is thankful to Professors P. Ring, D. Vretnar, N. Van Giai, W. P. Liu, Z. Y. Ma, and Dr. L. G. Cao for helpful discussions. This work was supported by the National Natural Science Foundation of China (Grant No. 10975190), the Major State Basic Research Development Program of China (Grant No. 2007CB815003), and the Funds for Creative Research Groups of China (Grant No. 11021504).

-
- [1] R. B. Wiringa, V. G. J. Stoks, and R. Schiavilla, *Phys. Rev. C* **51**, 38 (1995).
 - [2] R. Machleidt, *Phys. Rev. C* **63**, 024001 (2001).
 - [3] F. Stancu, D. M. Brink, and H. Flocard, *Phys. Lett. B* **68**, 108 (1977).
 - [4] R. B. Wiringa, V. Fiks, and A. Fabrocini, *Phys. Rev. C* **38**, 1010 (1988).
 - [5] M. Zalewski, P. Olbratowski, M. Rafalski, W. Satula, T. R. Werner, and R. A. Wyss, *Phys. Rev. C* **80**, 064307 (2009).
 - [6] C. L. Bai, H. Q. Zhang, H. Sagawa, X. Z. Zhang, G. Coló, and F. R. Xu, *Phys. Rev. Lett.* **105**, 072501 (2010).
 - [7] L. G. Cao, G. Coló, H. Sagawa, P. F. Bortignon, and L. Sciacchitano, *Phys. Rev. C* **80**, 064304 (2009); L. G. Cao, G. Coló, and H. Sagawa, *ibid.* **81**, 044302 (2010); L. G. Cao, H. Sagawa, and G. Coló, *ibid.* **83**, 034324 (2011).
 - [8] C. W. Wong, *Nucl. Phys. A* **108**, 481 (1968).
 - [9] J. W. Negele, *Phys. Rev. C* **1**, 1260 (1970).
 - [10] D. Vautherin and D. M. Brink, *Phys. Rev. C* **5**, 626 (1972).
 - [11] D. W. L. Sprung, *Nucl. Phys. A* **182**, 97 (1972).
 - [12] R. R. Scheerbaum, *Nucl. Phys. A* **257**, 77 (1976).
 - [13] T. H. R. Skyrme, *Philos. Mag.* **1**, 1043 (1956); *Nucl. Phys.* **9**, 615 (1959); **9**, 635 (1959).

- [14] J. S. Bell and T. H. R. Skyrme, *Philos. Mag.* **1**, 1055 (1956).
- [15] F. Tondeur, *Phys. Lett. B* **123**, 139 (1983).
- [16] K. F. Liu, H. D. Luo, Z. Y. Ma, Q. B. Shen, and S. A. Moszkowski, *Nucl. Phys. A* **534**, 1 (1991).
- [17] T. Otsuka, T. Suzuki, R. Fujimoto, H. Grawe, and Y. Akaishi, *Phys. Rev. Lett.* **95**, 232502 (2005).
- [18] T. Otsuka, T. Matsuo, and D. Abe, *Phys. Rev. Lett.* **97**, 162501 (2006).
- [19] T. Otsuka, T. Suzuki, M. Honma, Y. Utsuno, N. Tsunoda, K. Tsukiyama, and M. Hjorth-Jensen, *Phys. Rev. Lett.* **104**, 012501 (2010).
- [20] N. A. Smirnova, B. Bally, K. Heyde, F. Nowacki, and K. Sieja, *Phys. Lett. B* **686**, 109 (2010).
- [21] B. A. Brown, T. Duguet, T. Otsuka, D. Abe, and T. Suzuki, *Phys. Rev. C* **74**, 061303(R) (2006).
- [22] G. G. Coló, H. Sagawa, S. Fracasso, and P. F. Bortignon, *Phys. Lett. B* **646**, 227 (2007).
- [23] D. M. Brink and F. Stancu, *Phys. Rev. C* **75**, 064311 (2007).
- [24] W. Zou, G. Coló, Z. Y. Ma, H. Sagawa, and P. F. Bortignon, *Phys. Rev. C* **77**, 014314 (2008).
- [25] M. Moreno-Torres, M. Grasso, H. Liang, V. De Donno, M. Anguiano, and N. Van Giai, *Phys. Rev. C* **81**, 064327 (2010).
- [26] E. B. Suckling and P. D. Stevenson, *Eur. Phys. Lett.* **90**, 12001 (2010).
- [27] H. Nakada, *Phys. Rev. C* **81**, 051302(R) (2010).
- [28] Y. Z. Wang, J. Z. Gu, J. M. Dong, and X. Z. Zhang, *Phys. Rev. C* **83**, 054305 (2011).
- [29] A. Ozawa, T. Kobayashi, T. Suzuki, K. Yoshida, and I. Tanihata, *Phys. Rev. Lett.* **84**, 5493 (2000).
- [30] E. Becheva *et al.*, *Phys. Rev. Lett.* **96**, 012501 (2006).
- [31] Z. Elekes *et al.*, *Phys. Rev. Lett.* **98**, 102502 (2007).
- [32] B. G. Todd-Rutel, J. Piekarewicz, and P. D. Cottle, *Phys. Rev. C* **69**, 021301(R) (2004).
- [33] T. W. Burrows, *Nucl. Data Sheets* **74**, 1 (1995); J. S. Hanspal, N. M. Clarke, R. J. Griffiths, O. Karban, and S. Roman, *Nucl. Phys. A* **436**, 236 (1985); S. Fortier, E. Hourani, M. N. Rao, and S. Galés, *ibid.* **A311**, 324 (1978).
- [34] C. A. Ogilvie, D. Barker, J. B. A. England, M. C. Mannion, J. M. Nelson, L. Zybert, and R. Zybert, *Nucl. Phys. A* **465**, 445 (1987).
- [35] X. Campi and D. W. L. Sprung, *Phys. Lett. B* **46**, 291 (1973).
- [36] D. W. L. Sprung and P. K. Banerjee, *Nucl. Phys. A* **168**, 273 (1971).
- [37] M. Grasso, Z. Y. Ma, E. Khan, J. Margueron, and N. Van Giai, *Phys. Rev. C* **76**, 044319 (2007).
- [38] T. Lesinski, M. Bender, K. Bennaceur, T. Duguet, and J. Meyer, *Phys. Rev. C* **76**, 014312 (2007).
- [39] M. Bender, K. Bennaceur, T. Duguet, P. H. Heenen, T. Lesinski, and J. Meyer, *Phys. Rev. C* **80**, 064302 (2009).
- [40] E. Khan, M. Grasso, J. Margueron, and N. Van Giai, *Nucl. Phys. A* **800**, 37 (2008).
- [41] M. Bender, K. Rutz, P.-G. Reinhard, J. A. Maruhn, and W. Greiner, *Phys. Rev. C* **60**, 034304 (1999).
- [42] M. Grasso, L. Gaudefroy, E. Khan, T. Niksić, J. Piekarewicz, O. Sorlin, N. Van Giai, and D. Vretenar, *Phys. Rev. C* **79**, 034318 (2009).
- [43] M. Grasso *et al.*, *Int. J. Mod. Phys. E* **18**, 2009 (2009).
- [44] K. Bennaceur and J. Dobaczewski, *Comput. Phys. Commun.* **168**, 96 (2005).
- [45] J. Dobaczewski, J. Dudek, and P. Olbratowski, *Comput. Phys. Commun.* **158**, 158 (2004).
- [46] P. Bonche, H. Flocard, and P. H. Heenen, *Comput. Phys. Commun.* **171**, 49 (2005).
- [47] E. Chabanat, P. Bonche, P. Haensel, J. Meyer, and R. Schaeffer, *Nucl. Phys. A* **635**, 231 (1998).
- [48] P. D. Cottle and K. W. Kemper, *Phys. Rev. C* **58**, 3761 (1998).
- [49] A. Gade *et al.*, *Phys. Rev. C* **74**, 034322 (2006).